A Genetic Linkage Map of the Mouse: Current Applications and Future Prospects

Neal G. Copeland,* Nancy A. Jenkins, Debra J. Gilbert, Janan T. Eppig, Lois J. Maltais, Joyce C. Miller, William F. Dietrich, Alix Weaver, Stephen E. Lincoln, Robert G. Steen, Lincoln D. Stein, Joseph H. Nadeau, Eric S. Lander*

Technological advances have made possible the development of high-resolution genetic linkage maps for the mouse. These maps in turn offer exciting prospects for understanding mammalian genome evolution through comparative mapping, for developing mouse models of human disease, and for identifying the function of all genes in the organism.

Historically, the mouse has been the mammal of choice for genetic analysis primarily because of its short gestation period and large litter sizes, the availability of inbred strains, and the ability to perform controlled matings. The mouse has also served as an important model for human genetic diseases such as anemias, autoimmunity and other immune dysfunctions, neurological disorders, birth defects, cancer, diabetes, atherosclerosis, and various reproductive anomalies. In recent years, the development of transgenic and embryonic stem cell technology has made it possible to ectopically express virtually any gene in any mouse tissue and to create targeted germline gain-of-function and loss-of-function mutations. Just in the past year, the ability to introduce into the mouse germ line yeast artificial chromosomes that carry several hundred kilobases of genomic DNA has opened unparalleled opportunities for genome analysis and for the development of new mouse models of human disease. It is not surprising, therefore, that the goals of the Human Genome Project include the development of high-resolution genetic and physical maps of the mouse, leading to the eventual identification and functional characterization of all genes in the organism.

As with human genetic maps, mouse genetic maps serve two distinct goals. First, they provide a tool for genetic analysis and manipulation—including mapping of mutations causing biologically interesting traits, chromosomal localization of cloned genes, and the construction of animals with defined genotypes. Second, they facilitate the development of the physical map, providing a well-ordered scaffold onto which can be placed "contigs" of overlapping clones.

Gene mapping in the mouse began early in the first part of this century when J. B. S. Haldane, A. D. Sprunt, and N. M. Haldane reported in the *Journal of Genetics* that two coat color mutations, albino and pink-eyed dilution, were linked (*1*). Conceptually, mouse mapping changed little from the time of Haldane to the early 1970s and consisted primarily of genetic linkage analysis of phenotypic deviants. As a result, the pace of gene mapping proceeded relatively slowly, and the number of mapped loci roughly doubled every decade (*2*).

In situ hybridization and somatic cell genetics have been useful in the mouse, but these techniques have played a lesser role in mouse mapping than in human gene mapping. Both techniques rely on the ability to discriminate cytologically between chromosomes. This is difficult in the mouse because normal mouse chromosomes are all acrocentric (human chromosomes are metacentric) and show a continuous gradation in size. In addition, somatic cell hybrids that carry single mouse chromosomes or chromosomes with deletions or translocations are rare, which complicates subchromosomal gene assignments by this approach. Finally, and probably most importantly, it was usually possible in mice to find a variant that could be genetically mapped with a specific cross, which was not possible in humans.

The explosion in mouse gene mapping in recent years was sparked by the advent of new types of genetic markers. Recombinant DNA techniques allowed the identification and mapping of DNA polymorphisms (*3*), which have provided an abundant source of biologically interesting loci for the mouse map. DNA markers were initially scored as restriction fragment length polymorphisms (RFLPs) on Southern (DNA) blots; more recently, many have been developed that can be assayed by the polymerase chain reaction (PCR).

Interspecific Crosses

In addition to these new markers, the development of new types of crosses has played a key role in the dramatic explosion in mouse gene mapping. Until the mid-1980s, mouse gene assignments tended to rely on two- and three-point crosses between laboratory strains or recombinant inbred strains (*4*). However, these approaches are limited by the low degree of allelic variation among laboratory strains. Determining the overall order of genes in the mouse is also problematic if only a handful of genes are informative in any given cross; a composite map can be inferred only indirectly.

These problems were overcome with the use of interspecific crosses, which involve a laboratory strain and a distantly related species of *Mus*. Interspecific crosses exploit the genetic diversity inherent between wild mouse species and common laboratory strains. Most genes or DNA sequences are polymorphic in an interspecific cross and can thus be placed relative to other genes in a single interspecific cross. DNA from a single cross is sufficient to permit mapping of thousands of genes by RFLPs or tens of thousands of genes by PCR. Because many genes can be mapped simultaneously, gene order is easy to define, at least within a single cross. The use of interspecific crosses for mouse mapping was pioneered by Francois Bonhomme, Philip Avner, and Jean-Louis Guénet in the late 1970s and mid-1980s (*5, 6*). Since that time, many laboratories have developed and made use of interspecific crosses for mouse mapping, and now most mouse genes are mapped in interspecific crosses.

One of the most genetically divergent *Mus* species that still interbreeds with common laboratory mice to produce at least one sex that is fertile is *Mus spretus* (*6*). For this reason, *M. spretus* has become the mouse of choice for interspecific crosses. Notwithstanding its advantages, there are two drawbacks to using *M. spretus*: (i) F_1 males are

N. G. Copeland. N. A. Jenkins, and D. J. Gilbert are with the ABL–Basic Research Program, National Cancer Institute–Frederick Cancer Research and Development Center, Frederick, MD 21702. J. T. Eppig, L. J. Maltais, and J. H. Nadeau are with The Jackson Laboratory, Bar Harbor, ME 04609. J. C. Miller, W. F. Dietrich, A. Weaver, S. E. Lincoln, R. G. Steen, L. D. Stein, and E. S. Lander are with the Whitehead Institute for Biomedical Research, 9 Cambridge Center, Cambridge, MA 02142. E. S. Lander is also with the Department of Biology, Massachusetts Institute of Technology, Cambridge, MA 01239.

*To whom correspondence should be addressed.

sterile and thus only female F_1 mice can be used as parents in a backcross for gene mapping, which prevents the study of male meiosis; and (ii) the wide divergence between *M. spretus* and the laboratory mouse may have permitted the accumulation of small chromosomal inversions that could suppress recombination and possibly hamper the fine-structure genetic mapping needed in positional cloning. To overcome these limitations (or at least to hedge their bets), many laboratories have now started also using *Mus musculus castaneus* or *Mus musculus molossinus* as the wild mouse parent. These mice are somewhat more closely related to the laboratory mouse, belonging to the same species but a different subspecies. Both sexes are fertile in the F_1 progeny of such intersubspecific crosses. Moreover, the degree of polymorphism in such crosses is very high.

A problem that has not yet been fully resolved is how to combine mapping data generated by different laboratories using different crosses. A partial solution to this problem is to include a common set of anchor loci among the probes mapped in each cross. Mapping data can then be combined with respect to the anchor loci. Toward this end, the mouse mapping community has defined a common set of anchor loci for use in gene mapping. Anchor loci have been chosen to be evenly spaced every 10 to 20 centimorgans (cM) in the mouse genome, to be highly polymorphic within even intraspecific crosses, to be easily typed by PCR, and to be well mapped in interspecific crosses (*7*). Of course, although anchor data provide firm reference points between maps, the order of loci between the anchors can be only indirectly inferred on the basis of distances; such inferences can be unreliable because of variation in recombination frequencies among crosses.

The Mouse Genetic Map

Current genetic maps in mammals are generally composed of four types of loci: mutations that cause phenotypic deviations, isozyme loci, cloned genes, and highly polymorphic anonymous DNA segments. These categories overlap in some cases and will eventually merge as the entire mouse genome is mapped and cloned. Each type of locus plays an important role in genomic analysis. Mutant loci have been mapped throughout the century, and up-to-date maps have been published (*7*). Such maps point to biologically interesting genes but alone shed no light on the biochemical basis of the defect. Cloned genes provide important biological information and are especially useful in comparative mapping relating the mouse, human, and other mammalian genomes. However, gene probes can be tedious to genotype and are often not polymorphic in crosses between closely related strains. Highly polymorphic DNA segments—including minisatellites, microsatellites, and single-strand conformation polymorphisms—provide little biological information, but they are often informative in crosses between closely related strains and many can be rapidly mapped by PCR typing.

The wall chart that appears in this issue represents the integration of two DNA marker maps: a gene-based map with 1098 loci, which focuses on mouse-human comparative mapping, and a simple sequence length polymorphism (SSLP) or microsatellite map containing 1518 loci. Many genes and anonymous markers mapped in the mouse but not in humans have been omitted from the chart because of space constraints. The map shows many newly reported loci and also presents the first integration of these two mouse maps.

Gene-based map. The framework for the gene-based map is an interspecific backcross map being developed at Frederick, Maryland (*8*), which consists of the loci shown in black on the chart. The Frederick map was generated from crosses of (C57BL/6J × *M. spretus*)F_1 × C57BL/6J mice. Cloned DNA probes were hybridized to Southern blots of DNA from the two parental strains digested with a variety of restriction enzymes to identify RFLPs. The probes were then hybridized to Southern blots of restriction-digested DNAs from the backcrossed mice in order to follow the inheritance of *M. spretus*–specific RFLP alleles in the progeny. For the construction of the map, the progeny were first typed for a series of markers whose positions had been accurately established on the mouse linkage map in other laboratories. These loci served as anchors for placing new genes on the evolving map. As each additional probe was mapped, the gene order was determined by comparing the new RFLP segregation patterns to the known patterns and finding the position that minimized the number of crossovers required to explain the new segregation pattern. Because all the loci were mapped in a single backcross, the relative position of each of these loci was established with a high degree of confidence. The gene orders are supported by a likelihood ratio of 1000:1, except for underlined loci whose position is less well established. Underlined loci represent loci for which key recombinant animals have not yet been typed. Mouse nomenclature is in flux and the chart conforms to our understanding of the manner in which the databases are being changed.

In total, the current Frederick map contains over 1300 loci distributed over all mouse chromosomes; the map on the chart shows 643 of these loci. Virtually all loci, both published and unpublished, that have also been mapped in the human genome (indicated in bold type) are included because the gene-based map is meant to emphasize the current state of human-mouse comparative mapping. One hundred eighty-one additionally published loci mapped at Frederick that have not yet been mapped in the human genome are also included to help in integrating the Massachusetts Institute of Technology (MIT) SSLP map with the Frederick map (indicated in regular black type). Finally, the chart also contains virtually all additional genes and DNA segments that have been mapped in the human and the mouse genomes (but not in the Frederick cross) as reported in the 1993 Mouse Chromosome Committee Reports (indicated in red type) (*7*). A few DNA segments, particularly those mapping in the proximal region of mouse chromosome 17, were omitted from the chart because of space constraints. The loci reported in the committee reports were mapped by many different laboratories using a variety of different techniques (*7*). Because these loci were mapped in many different crosses, the position of these loci on the Frederick framework map can be only indirectly inferred from available mapping information. The locations of these loci on the map should thus be considered provisional.

The Frederick framework map shown in the chart has been aligned with respect to the centromere by mapping various proximal loci (indicated by brackets) in a separate interspecific cross in which the inheritance pattern of cytologically visible subcentromeric repeats had been established (*9*). Because the mapping was performed in a separate cross, the distances are not perfectly comparable and, for a few chromosomes, some appear to extend 1 to 3 cM beyond the centromere. When telomere probes are developed, it will be possible to define the complete extent of the genetic map.

SSLP map. The SSLP map consists of polymorphic genetic markers defined by PCR assays, each involving a specific pair of primers flanking the site of a di-, tri- or tetranucleotide repeat sequence having a variable length in differing mouse strains. SSLPs or microsatellite polymorphisms were first described by Weber and May (*10*) in humans and were first studied by Todd and colleagues (*11*) in mice. They have rapidly become a genetic marker of choice for mammalian genetics for a number of reasons, including the ease of finding such markers [the most frequent simple sequence repeat in mammalian genomes is $(CA)_n$, which occurs roughly 100,000 times in the mouse genome with an average spacing of 1 every 30 kb], their high rate of polymor-

phism even among closely related individuals and strains, and the fact that they can be disseminated by simply publishing the primer sequence.

The SSLP map shown in the chart is the result of an ongoing project (*12*) at the Whitehead Institute/MIT Center for Genome Research (WI/MIT-CGR) aimed at building a dense genetic and physical map of the mouse genome. Most of the genetic markers are $(CA)_n$ repeats. Some 90% of the markers were developed by screening a small-insert library of mouse genomic DNA to find $(CA)_n$ repeat–containing clones, determining their DNA sequence, and choosing PCR primers flanking the repeat (with the use of a computer program designed to identify primers that would work under uniform PCR conditions). The remaining 10% were based on simple sequence repeats that occurred in published gene sequences and thus are gene-based markers. All the simple sequence repeats were tested for polymorphism among 12 inbred mouse strains. Overall, they showed a polymorphism rate of about 90% in interspecies or intersubspecies comparisons and a polymorphism rate of about 50% in intraspecies comparisons. Thus, these highly polymorphic markers are suitable for typing virtually any mouse cross, whether interspecific or among laboratory strains.

The SSLPs were all genotyped in a single (C57BL/6J-*ob* × CAST/Ei)F_2 intersubspecific cross (CAST/Ei is a strain of *M. m. castaneus*). The genetic map was built by analyzing the inheritance patterns with the MAPMAKER computer program (*13*); for this, those SSLPs taken from genes with known chromosomal position served as anchors for alignment with the previous mouse maps. Because all the loci were analyzed in a single cross, their relative positions were established with a high degree of confidence. The gene orders are supported by a likelihood ratio of 1000:1, except for underlined loci whose position is less well established. These underlined loci represent markers for which there is not full genotypic information. The data were subjected to a mathematical error-checking procedure (*14*) to identify likely typing errors and have been extensively rechecked. Because the mapping cross involved only about 100 meioses, markers are clustered in "bins" whenever no crossovers occurred in the meioses studied; the fine-structure order of these markers can be established by studying more meioses or by physical mapping. The spacing between markers is reasonably close to random, although mathematical tests can detect a small but statistically significant excess of larger intervals that may correspond to recombinational hotspots.

The SSLP map in the chart showing 1518 loci was current as of 1 July 1993. As this article goes to press, the total number of SSLP loci is already more than 2000. Taking advantage of the ability to distribute SSLPs simply by publishing their sequence, WI/MIT-CGR maintains an electronic mail (e-mail) server to provide up-to-date information about the map, including the locations, primer sequences, and allele sizes of all SSLPs. In addition, GenBank names for SSLP markers taken from GenBank are available via the e-mail server. To obtain an e-mail query form and instructions, send an e-mail message with the single word *help* to genome_database@genome.wi.mit.edu.

Integration and comparison of maps. The two maps play complementary roles in mouse genetics: the SSLP map provides markers now routinely used for the genetic analysis of crosses, whereas the gene-based map shows the known genes in a region, thereby suggesting likely candidate genes for a mutation and indicating correspondence to the human genome. With the aim of merging this information into a single comprehensive view of the mouse genome, the Frederick and Whitehead groups recently undertook a project to integrate the two maps. In order to do so, 254 of the SSLPs developed at WI/MIT-CGR were genotyped in a subset of 46 progeny from the Frederick interspecific backcross. SSLP markers that were relatively well spaced throughout the mouse genome were chosen for the integration. On the basis of their inheritance patterns, the SSLPs could be assigned to intervals in the Frederick map that were defined by the closest flanking crossovers in the progeny scored—typically, a region of about 2 cM. Although this does not establish fine-structure local order, it establishes 254 ties between the two maps (shown by green lines connecting the SSLP map with the chromosome diagram in the center)—roughly one SSLP marker every 6 cM.

It is interesting to compare certain features of the maps, such as genetic length. The genetic length of the mouse genome has been estimated to be about 1600 cM, and the chromosome lengths in the chart are drawn to scale on the basis of this estimate. However, the frequency of recombination between loci is not constant but may depend on the cross and the sex of the individual in which meiosis occurs (*15*). Overall, although not thoroughly examined for mice, recombination distances appear larger in female than male meiosis, but for some chromosomal regions male recombination distances are greater (*16*).

In the Frederick cross, the total genetic length is estimated to be only about 1350 cM. Given the large number of markers on the map, the Frederick map would be expected to cover nearly the entire genome. Yet, each chromosome appears shorter than predicted, with the exception of chromosome 11. The discrepancy may be even greater than it seems because genetic distance was measured only in female meiosis, which shows more recombination as a rule. It is possible that small inversions and other rearrangements between C57BL/6J and *M. spretus* chromosomes may suppress recombination and result in a smaller map, although only one instance of a structural difference has been documented so far, a small inversion in the proximal region of *M. spretus* chromosome 17 (*17*). In the SSLP map, the genetic length is somewhat larger, although still less than 1600 cM. The total length is estimated to be about 1450 cM, with genetic distances in this cross representing the average of male and female meiosis in an intersubspecific cross. There may also be some recombinational suppression in this cross as well. Alternatively, it may be that the conventional estimate of 1600 cM is simply 10% too high.

Closer comparison suggests possible regions of recombinational suppression. One clear example is the interval from D5Mit19 to D5Mit68, which measured 24 cM in the SSLP cross but was compressed to only 6 cM in the Frederick cross; this would be consistent with the occurrence of a small inversion within this interval in *M. spretus* compared to C57BL/6J and CAST/Ei. More thorough examination of recombinational suppression will require typing markers in various interspecific, intersubspecific, and intraspecific crosses. Fluorescence in situ hybridization may then prove useful in confirming candidate inversions.

Transmission ratio distortion, the occurrence of non-Mendelian ratios for some loci, is often observed in interspecific crosses in animals and plants. In the mouse, it was first reported in a (C3H/HeHa × *M. spretus*)F_1 × *M. spretus* backcross in which there was a deficiency of backcross males carrying the intact X chromosome from C3H/HeHa (*18*). The mechanism (or mechanisms) responsible for transmission ratio distortion are not understood but may result from differential embryo survival because of different combinations of progenitor strain alleles. In the Frederick (C57BL/6J × *M. spretus*) interspecific backcross, transmission ratio distortion was observed for chromosomes 2, 4, and 10 (*19*), with the distortion consistently involving an excess of *M. spretus* alleles relative to C57BL/6J alleles inherited by backcross mice. By contrast, the (C57BL/6J × CAST/Ei) intersubspecific intercross showed no statistically significant evidence of transmission distortion. It is not clear whether this difference reflects greater incompatibility between C57BL/6J and *M. spretus* alleles, but the mapping and cloning of the loci that cause the transmission ratio distortion seem feasible.

Applications of the Map

Mouse maps, such as those depicted on the chart, have many different applications for genome research. Although their uses are too numerous to outline here, we highlight here some of the more important applications of the maps for current and future genome research.

Comparative mapping. Of the 2616 loci listed in the chart, 917 have homologs that have been mapped in humans (Table 1). These loci mark 101 segments of conserved linkage homology. On the chart, these conserved linkages are shown as colored segments within each chromosome map, and a summary of these results is shown in Fig. 1. The total length of all conserved autosomal segments is 911 cM, which indicates that ~61% of the genome is already accounted for in the current comparative map. Correcting for the fact that these conserved segments extend some distance beyond their current bounds (*20*), we estimate that approximately 1194 cM, or 80% of the mouse autosomal genome, is accounted for in the comparative map.

In 1984, Nadeau and Taylor calculated that the average length of a conserved autosomal segment in mice is ~8.1 cM (*20*). This calculation was based on 83 homologous loci marking 13 conserved segments and on several assumptions concerning the distribution of recombination and rearrangement breakpoints. By applying the same calculation to the map shown in the chart, which represents roughly a ~15-fold increase in data, the current average length of a conserved autosomal segment is 8.8 cM, which is not statistically different from the previous estimate. This remarkable consistency strongly suggests that the assumptions that underlie the calculation are correct.

Several examples exist of linkage conservation across a human centromere—for example, the region of human chromosome 20 homology on mouse chromosome 2 and the region of human chromosome 17 homology on mouse chromosome 11. Whether these represent ancestral linkages or derived rearrangements remains to be determined through more detailed comparative mapping studies.

The large number of conserved segments shown in the current map suggest that multiple chromosomal rearrangements have occurred since the divergence of the lineages leading to humans and mice. On the basis of the data in the chart, we calculate that approximately 150 rearrangements have occurred since this divergence (*20*). These rearrangements likely have occurred through several different mechanisms, including chromosome translocations, inversions, insertions, and other complex rearrangements. Such rearrangements have even led to changes in gene order within conserved segments (Table 1).

An important application of the comparative map is the transfer of linkage information and genome resources from "map-rich" to "map-poor" species (*21, 22*). By mapping a well-defined set of evolutionarily conserved loci across mammalian genomes, it should be possible to use these conserved loci as reference points to transfer linkage information from "map-rich" species such as humans and mice to "map-poor" species such as cow, pig, and sheep and thereby expedite genome research. This is somewhat analogous to using anchor loci to combine linkage data within a single species. Such a set of reference loci for comparative mapping in mammals was recently proposed (*22*).

Another important application of the comparative map involves analysis of complex traits. Susceptibility to many important genetic disorders is controlled by more than one gene, and the identification of these genes is often easier in mice than in humans. Once a candidate disease gene or disease region is identified in the mouse, the homologous genes or regions in humans can be screened to see if they are linked to the corresponding human genetic disease.

Genome evolution and the origin of multigene families. Multigene families are thought to be generated by a number of different mechanisms. These include (i) reverse transcription, a process likely responsible for pseudogene formation; (ii) tandem gene duplication, which is thought to arise from unequal crossing-over; and (iii) genome duplication. Genome duplication could involve chromosomal segment duplication, chromosome duplication, or whole genome duplication. It is believed that the eukaryotic genome has undergone multiple genome duplication events, with the most recent duplication event occurring approximately 300 million years ago, long before the divergence of the lineages leading to the mouse and human genomes (*23*). As more and more multigene families are mapped in the mouse as well as other mammalian species, it should be possible to begin to piece together the nature of the events giving rise to multigene families. Like traditional comparative maps, maps of duplicated or paralogous chromosomal segments can also be used to predict linkages and identify candidate disease genes.

A recent example of the power of the mapping approach for the study of the evolution of mammalian multigene families can be found in Wilkie *et al.* (*24*), who studied the evolution of the mammalian Gα protein subunit multigene family. In this study, Wilkie and co-workers showed that members of two of the four subclasses, G_{12} and G_s, of Gα protein subunit genes probably arose by successive genome duplication of a single Gα progenitor gene, whereas members of the G_i and G_q subclasses probably arose from successive genome duplication of a tandem Gα gene pair. Another excellent example of such map-

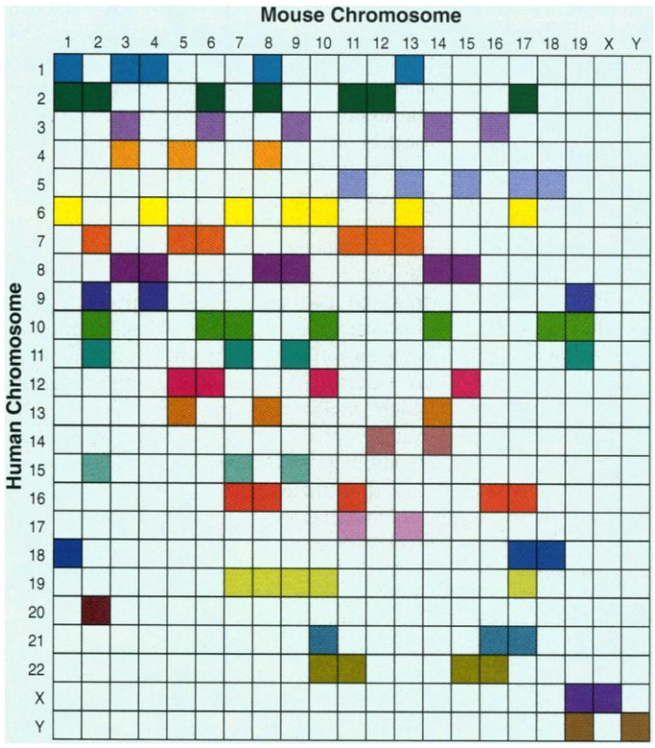

Fig. 1. The Oxford grid showing the locations of homologous genes and anonymous loci in humans and mice. Each colored cell in the matrix indicates at least one locus that has been mapped to the respective chromosome in both the mouse and human genomes.

Table 1. Human chromosomal location of genes and anonymous DNA loci mapped in both humans and mice.

Mouse Symbol	Human Symbol	Human Location
	Chromosome 1	
Col9a1	COL9A1	6q12-q14
Bpag1	BPAG1	6p12-p11
Il1r1	IL1RA	2q12
Col3a1	COL3A1	2q31-q32.3
Gls	GLS	2q32-q34
Ctla4	CTLA4	2q33
Cd28	CD28	2q33
dh1	IDH1	2q32-qter
Creb1	CREB1	2q32-q34
Mtap2	MAP2	2q34-q35
Cryg	CRYGA	2q33-q35
Mylf	MYL1	2q32.1-qter
Fn1	FN1	2q34-q36
Tnp1	TNP1	2q35-q36
Vil	VIL1	2q35-q36
Inha	INHA	2q33-qter
Des	DES	2q35
Ugt1a1	UGT1A1	2q37
Pax3	PAX3	2q35-q37
Acrg	CHRNG	2q32-qter
Col6a3	COL6A3	2q37
Acrd	CHRND	2q33-qter
Akp3	ALPI	2q34-q37
Sag	SAG	2q24-q37
Bcl2	BCL2	18q21.3
Planh2	PLANH2	18q21.3
Inhbb	INHBB	2cen-q13
En1	EN1	2q13-q21
C4bp	C4BPA	1q32
Ren1	REN	1q32
Il10	IL10	1
Atp2b4	ATP2B4	1q25-q32
Pep3	PEPC	1q25
Myog	MYOG	1q31-q41
Cd45	PTPRC	1q31-q32
Cfh	HF1	1q32
Ncf2	NCF2	1cen-q32
Lamb2	LAMB2	1q31
Abll	ABL2	1q24-q25
At3	AT3	1q23-q25.1
Sele	SELE	1q22-q25
Cf5	F5	1q21-q25
Atp1b1	ATP1B1	1q22-q25
Selp	SELP	1q22-q25
Sell	SELL	1q23-q25
Otf1	OTF1	1cen-q32
Cd3z	CD3Z	1q22-q25
Pbx1	PBX1	1q23
Rxrg	RXRG	1q23-q25
Fcgr2	FCGR2A	1cen-q32
Fcgr3	FCGR3	1q23
Mpp	MPP	1q21-q23
Apoa2	APOA2	1q21-q23
Cd48	CD48	1q21.3-q22
Fcer1g	FCER1G	1q23
Atpla2	ATP1A2	1q21-q23
Crp	CRP	1q21-q23
Fcer1a	FCER1A	1q23
Sap	APCS	1q23
Spna1	SPTA1	1q21
Adprp	ADPRT	1q41-q42
Eph1	EPHX	1p11-qter
Tgfb2	TGFB2	1q41
Cd34	CD34	1q12-qter
Cr2	CR2	1q32
Mcp	MCP	1q32
	Chromosome 2	
Itih2	ITIH2	10p15
Gata3	GATA3	10p15
Vim	VIM	10p13
Bmi1	BMI1	10
Gad2	GAD2	10p13-p11.2
Il1rn	IL1RN	2q14.2
Pax8	PAX8	2q
Surf	SURF1	9q33-q34
Tan1	TAN1	9q34.3
Dbh	DBH	9q34.3
Spna2	SPTAN1	9q34.1
Ass1	ASS	9q34.1
Ab1	ABL1	9q34.1
Ak1	AK1	9q34.1
D2H9S46E	D9S46E	9q34
Hc	C5	9q33
Grp78	GRP78	9q33-q34.1
Gsn	GSN	9q33
His1	VIS1	2q14-q21
Neb	NEB	2q31-q32
Itgb6	ITGB6	2
Scn2a	SCN2A	2q23
Scn3a	SCN3A	2q23
Gcg	GCG	2q36-q37
Itga6	ITGA6	2
Gad1	GAD1	2q31
Acra	CHRNA1	2q24-q32
Creb1	CREB1	2q32-q34
Hoxd	HOXD	2q31-q37
Evx2	EVX2	2q31-q32
Dlx2	DLX2	2cen-q33
Itga4	ITGA4	2q31-q32
Itgav	ITGAV	2q31-q32
Sfpi1	SPI1	11p12-p11.2
Cf2	F2	11p11-q12
Rag1	RAG1	11p13
D2Hgu1	D11S102	11p13
Rag2	RAG2	11p13
Cd44	CD44	11p13
Cas1	CAT	11p13
Wt1	WT1	11p13
Pax6	PAX6	11p13
Fshb	FSHB	11p13
Kcna4	KCNA4	11p14
Rbtn2	RBTNL1	11p13
Bdnf	BDNF	11p13
Blvr	BLVR	7p14-cen
Actc1	ACTC	15q11-qter
Sgne1	SGNE1	15q13-q14
Id	FMN	15q13.3-q14
Thbs1	THBS1	15q15
Sdh1	SORD	15pter-q21
Ltk	LTK	15
Epb4.2	EPB42	15q15
B2m	B2M	15q21-q22.2
Hdc	HDC	15
Il1a	IL1A	2q12-q21
Il1b	IL1B	2q13-q21
Glvr1	GLVR1	2q11-q14
Pdyn	PDYN	20pter-p12
Prn	PPRNP	20pter-p12
Snrpb	SNRPB	20
Avp	AVP	20p13
Oxt	OXT	20p13
Itp	ITPA	20p
Pcna	PCNA	20pter-p12
Chgb	CHGB	20pter-p12
Bmp2	BMP2	20p12
Nec2	NEC2	20p11.2
Pax1	PAX1	20p11.2
Thbd	THBD	20p12-cen
Pygb	PYGB	20p
Hck	HCK	20q11-q12
Ghrf	GHRH	20p12 or 20q11.2-q12
Ahcy	AHCY	20cen-q13.1
Src	SRC	20q11.2-q13
Rpn2	RPN2	20q12-q13
Top1	TOP1	20q12-q13.1
Plcg1	PLC1	20q12-q13.1
Ada	ADA	20q12-q13.11
Cebpb	CEBPB	20q13.1
Pck1	PCK1	20q13.31
Gnas	GNAS1	20q13.2-q13.3
Acra4	CHRNA4	20
	Chromosome 3	
Il7	IL7	8q12-q13
Crh	CRH	8q13
Car1	CA1	8q13-q22.1
Car2	CA2	8q13-q22.1
Car3	CA3	8q13-q22
Glut2	GLUT2	3q26.1-q26.3
Evi1	EVI1	3q24-q28
Fim3	FIM3	3q27
Ccna	CCNA	4q25-q31
Fgf2	FGF2	4q25-q27
Il2	IL2	4q26-q27
Mme	MME	3q21-q27
Glur2	GLUR2	4q25-q34.3
Fgg	FGG	4q28
Rnulb1	RNU1	1p36.1
Cacy	CACY	1q21-q25
Capl	CAPL	1q12-q21
Fcgr1	FCER1G	1q23
Fdpsl1	FDPSL1	1q24-q31
Gba	GBA	1q21
Pklr	PKLR	1q21
Ntrk1	NTRK1	1q23-q31
Lmna	LMNA	1cen-q32
Il6r	IL6R	1q21
Lor	LOR	1q21
Cdla	CD1A	1q22-q23
Flg	FLG	1q21
Hist2	H3F2	1q21
Gja5	GJA5	1p36-q12
Cd2	CD2	1p13
Hsd3b	HSDB3	1p13.1
Tshb	TSHB	1p13
Nras	NRAS	1p13
Ngfb	NGFB	1p13
Ampd1	AMPD1	1p13
Atpla1	ATP1A1	1p13
Rap1a	RAP1A	1p13.3
Cd53	CD53	1p31-p12
Gnai3	GNAI3	1p13
Gnat2	GNAT2	1p13
Csfm	CSF1	1p21-p13
Amy2	AMY2	1p21
Amy1	AMY1	1p21
Cf3	F3	1p22-p21
Vcam1	VCAM1	1p32-p31
Pxmp1	PXMP1	1p22-p21
Fabpi	FABP2	4q28-q31
Ank2	ANK2	4q25-q27
Egf	EGF	4q25
Nfkb1	NFKB1	4q24
Adh1	ADH1	4q21-q23
Adh3	ADH3	4q21-q23
Rpe65	RPE65	1p31
	Chromosome 4	
Lyn	LYN	8q13
Mos	MOS	8q11
Calb1	CALB1	8q21.3-q22.1
Cga	CGA	6q14-q21
Pax5	PAX5	9p13
Ggtb	GGTB2	9p21-p13
Galt	GALT	9p13
Tal1	TAL2	9q31-q32
Aco1	ACO1	9p22-q32
Cd72	CD72	9p
Lv	ALAD	9q32-q34
Orm1	ORM1	9q32
Orm2	ORM2	9q32
Hxb	HXB	9q32-q34
Cd30l	CD30L	9q33
Tyrp	TYRP	9p23
Ifa	IFN1	9p22
Ifb	IFNB1	9p22
Jun	JUN	1p32-p31
Pgm2	PGM1	1p22.1
C8b	C8B	1p32
Tal2	TAL1	1p32
Cyp4a	CYP4B1	1p34-p12
Urod	UROD	1p34
Glut1	GLUT1	1p35-p31.3
Ssbp	SSBP	1p
Lmyc1	MYCL1	1p32
Gja4	GJA4	1p36-q12
Csfgr	CSF3R	1p35-p34.3
Col8a2	COL8A2	1p34.3-p32.3
Lck	LCK	1p35-p32
Fgr	FGR	1p36.2-p36.1
Lag	LAP18	1p36.1-p35
Elp1	EPB41	1p34.2-p33
Fuca	FUCA1	1p35-p34
Htrld	HTR1D	1p36.3-p34.3
Akp2	ALPL	1p36.1-p34
Pnd	PND	1p36
Tnfr2	TNFR2	1p36.3-p36.2
Eno1	ENO1	1p36
Ski	SKI	1q22-q24
Pgd	PGD	1p36.3-p36.13
Gnb1	GNB1	1p36-p31.2
	Chromosome 5	
Gnai1	GNAI1	7q21-q22
Hgf	HGF	7q21.1
Pgy1	PGY1	7q21
Pgy3	PGY3	7q21
Sri	SRI	7
En2	EN2	7q36
Il6	IL6	7p21-p15
Fgfr3	FGFR3	4p16.3
D5H4S43	D4S43	4p16.3
Msx1	MSX1	4p16.3-p16.1
D5H4S115	D4S115	4p16.3
Drd5	DRD5	4p15.3-p15.1
D5H4S62	D4S62	4p16.2-16.1
Qdpr	QDPR	4p15.3
D5H4S76	D4S76	4p16.2-15.1
D5H4S80	D4S80	4p16.2-15.1
Idua	IDUA	4p16.3
Pep7	PEPS	4p11-q12
Pgm1	PGM2	4p14-q12
Gabrb1	GABRB1	4p13-p12
Gabra2	GABRA2	4p13-p12
Cncg	CNCG	4p14-p13
Pdgfra	PDGFRA	4q11-q12
Kit	KIT	4p11-q22
Flk1	KDR	4q12
Csnb	CSN2	4pter-q21
Alb1	ALB	4q11-q13
Afp	AFP	4q11-q13
Mgsa	GRO1	4q21
Bmp3	BMP3	4p14-q21
Fgf5	FGF5	4q21
Pdeb	PDEB	4p16.3
Spp1	SPP1	4q11-q21
Tcf1	TCF1	12q24.3
Bcd1	ACADS	12q22-qter
Gus	GUSB	7q22
Cyp3	CYP3	7q21.3-q22.1
Zp3	ZP3A	7
Epo	EPO	7q21.3-q22.1
Gnb2	GNB2	7q21.3-q22.1
Ache	ACHE	7q22
Mor1	MDH2	7cen-q22
Pdgfa	PDGFA	7p22
Flt3	FLT3	13q12
Flt1	FLT1	13q12
Atrc1	ATRC1	13q12.3
	Chromosome 6	
Cola2	COL1A2	7q21.3-q22.1
Tac2	TAC2	7q21-q22
Met	MET	7q31
Wnt2	WNT2	7q31
Cftr	CFTR	7q31.3
Cpa	CPA1	7q32
Pax4	PAX4	7q22-qter
Cald1	CALD1	7q33-q34
Ptn	PTN	7q33-q34
Braf	BRAF	7q34
Try1	TRY1	7q32-qter
Tcrb	TCRB	7q35
Clc1	CLCN1	7q32-qter
Evx1	EVX1	7p15-p14
Npy	NPY	7pter-q22
Hoxa	HOXA	7p15-p14
Ggc	GCTG	7pter-p14
Igk	IGKC	2p12
Cd8a	CD8A	2p12
Cd8b	CD8B1	2p12
Fabp1	FABP1	2p11
Sftp3	SFTP3	2
Tgfa	TGFA	2p13
Il5r	IL5RA	3p26-p24
Rho	RHO	3q21-q24
Raf1	RAF1	3p25
Itpr1	ITPR1	3p
Alox5	ALOX5	10
Ret	RET	10q11.2
M6pr	M6PR	12
Glut3	GLUT3	12p13.3
Gnb3	GNB3	12p13
Cd27	CD27	12p13
Tnfr1	TNFR1	12p13
Hcph	PTPN6	12p13
Cd4	CD4	12pter-p12
Tpi	TPI1	12p13
Vwf	VWF	12p13.3-p13.2
Gapd	GAPD	12p13
Fgf6	FGF6	12p13
Ccnd2	CCND2	12p13
Ntf3	NTF3	12p13
Prp	PRH1	12p13.2
Ldh2	LDHB	12p12.2-p12.1
Iapp	IAPP	12p12.3-p11.2
Rbtn3	RBTN3	12p13
Kras2	KRAS2	12p12.1
Pthlh	PTHLH	12p12.1-p11.2
	Chromosome 7	
Pvs	PVS	19q13.2
Zfp36	ZFP36	19q13.1
Pkcc	PRKCG	19q13.4
D7H19S51	D19S51	19q13.3
Tgfb1	TGFB1	19q13.1
Otf2	OTF2	19
Cea	CEA	19q13.2
Cyp2a	CYP2A	19q13.2
Cyp2b	CYP2B	19q13.2
D7H19S19	D19S19	19q13.2
Xrcc1	XRCC1	19q13.2
Ckmm	CKM	19q13.3
Apoe	APOE	19q13.2
Atpla3	ATP1A3	19q13.2
Ercc2	ERCC2	19q13,3
D7H19F11S1	D19F11S1	19q13.1
Gpi1	GPI	19q13.1
Cebp	CEBPA	19q13.1
Mag	MAG	19q13.1
Cd22	CD22	19q13.1
Ryr	RYR1	19q13.1
Bcl3	BCL3	19q13.1-q13.2
Pep4	PEPD	19q12-q13.2
Hrc	HRC	19q13.2-q13.3
Kal	KLK1	19q13.3
Rras	RRAS	19q13.3-qter
Lhb	LHB	19q13.3
Snrp70	SNRP70	19q13.3
Ntf5	NTF5	19
Kcnc1	KCNC1	11p15
Myod1	MYOD1	11p15
Ldh1	LDHA	11p15.1-p14
Ldh3	LDHC	11p15.5-p14.3
Tph	TPH	11p15.1-p14.3
Saa	SAA	19q13.1
p	P	15q11-q12
D7Nic2	D15F3751	15q11-q13
Gabrb3	GABRB3	15q11.2-q13
Snrpn	SNRPN	15q11-q13
Gabra5	GABRA5	15q11-q13
D7H15S9	ZNF127	15q11-q12
Igf1r	IGF1R	15q25-qter
Fur	PACE	15q25-q26
Fes	FES	15q25-qter
Fah	FAH	15q23-q25
Idh2	IDH2	15q21-qter
Tyr	TYR	11q14-q21
Mod2	ME2	6p25-p24
Omp	OMP	11q14-q21
Pth	PTH	11p15.2-p15.1
Rbtn1	RBTN1	11p15
Calc	CALCA	11p15.2-p15.1
Hbb	HBB	11p15.5
Pkcb	PRKCB	16p12
Il4r	IL4R	16p12.1-p11.2
Spn	SPN	16p11.2
Fgfr2	FGFR2	10q25.3-q26
Oat	OAT	10q26
Cyp2e1	CYP2E	10
Mgmt	MGMT	10q26
Ins2	INS	11p15.5
Th	TH	11p15.5
H19	D11S813E	11p15.5
Igf2	IGF2	11p15.5
Hras1	HRAS	11p15.5
Fgf3	FGF3	11q13
Fgf4	FGF4	11q13.3
Ccnd1	CCND1	11q13
Drd4	DRD4	11p15.5
	Chromosome 8	
Atp4b	ATP4B	13q34
Insr	INSR	19p13.3
Fcer2a	FCER2	19p13.3
Polb	POLB	8p12-p11

Mouse Symbol	Human Symbol	Human Location
Ank1	ANK	8p21.1-p11.2
Plat	PLAT	8p12-q11.2
Flt2	FGFR1	8p12
Defcr	DEF1	8p23-p22
Gr1	GSR	8p21.1
Scvr	SCVR	8
Lpl	LPL	8p22
Vpp3	VPP3	2cen-q13
Jund	JUND	19p13.2
Mel	MEL	19p13.1
Ucp	UCP	4q28-q31
Lyl1	LYL1	19p13.2
Junb	JUNB	19p13.2
Ces1	CES1	16q13-q22.1
Es6	ESB3	16
Mt1	MT1A	16q13
Mt2	MT2A	16q13
Mt3	MT3	16q13
Got2	GOT2	16q12-q22
Acadm	ACADM	1p31
Mov34	MOV34	16q23-q24
Um	UVO	16q22.1
Lcat	LCAT	16q22.1
Hp	HP	16q22.1
Ctrb	CTRB1	16q23-q24.1
Tat	TAT	16q22.1
Maf	MAF	16q22-q23
Aprt	APRT	16q24.2-qter
Cdh3	CDH3	16q24.1-qter
Acta2	ACTA1	1p21-qter
Agt	AGT	1q42-q43
	Chromosome 9	
Mmel	MMEL	11q22-q23
Il1bc	IL1BC	11q23
Ldlr	LDLR	19q13.2
Olfr2	OLFR2	19p13.1-p13.2
Epor	EPOR	19p13.2
Dnmt	DNMT	19p12.3-p12.2
Penk	PENK	8q11.23-q12
Icam1	ICAM1	19p13.2
Glur4	GLUR4	11q22
Appl	APPL	11
Ets1	ETS1	11q23.3
Fli1	FLI1	11q23-q24
Es17	ESA4	11q
Thy1	THY1	11q22.3-q23
Mll	MLL	11q23
Cbl2	CBL2	11q23.3-qter
Cd3g	CD3G	11q23
Cd3d	CD3D	11q23
Cd3e	CD3E	11q23
Ups	HMBS	11q23.2-qter
Drd2	DRD2	11q22-q23
Apoa1	APOA1	11q23-q24
Apoa4	APOA4	11q23-qter
Ncam	NCAM	11q23-q24
Hexa	HEXA	15q23-q24
Crabp1	CRABP1	15q22-qter
Cyp1a2	CYP1A2	15
Cyp1a1	CYP1A1	15q22-q24
Cyp11a	CYP11A	15q23-q24
Cyp19	CYP19	15q21
Csk	CSK	15q23-q25
Mpi1	MPI	15q22-qter
Acra5	CHRNA5	15q24
Cal1h	CAL1H	15q21-q22
Pk3	PKM2	15q24-q25
Acra3	CHRNA3	15q24
d	N.A.	15q15-q24
Htr1b	HTR1B	6q13
Bmp5	BMP5	6
Col12a1	COL12A1	6
Gsta	GSTA2	6p12.2
Mod1	ME1	6q12
Pgm3	PGM3	6q12
Rbp1	RBP1	3q21-q22
Rbp2	RBP2	3p11-qter
Trf	TF	3q21
Gnat1	GNAT1	3p21
Gnai2	GNAI2	3p21
Hgfl	MST1	3p21
Acy1	ACY1	3p21.1
Mylc	MYL3	3p21
Ltf	LTF	3p21
Col7a1	COL7A1	3p21
Bgl	GLB1	3p23-p22
Cck	CCK	3pter-p21
Nktr	NKTR	3p23-p21
	Chromosome 10	
Dmdl	UTRN	6q24
Pcmt1	PCMT1	6q22.3-q24
Estr	ESR	6q24-q27
Ifgr	IFNGR1	6q23-q24
Myb	MYB	6q22-q23
Ly41	M6S1	6q22-q23
Macs	MACS	6q21-q27
Col10a1	COL10A1	6q21-q22
Fyn	FYN	6q21
Ros1	ROS1	6q21-q22
Gja1	GJA1	6q14-qter
Hk1	HK1	10q22
Cdc2a	CDC2	10q21.1
Pfp	PRF1	10q22
Bcr	BCR	22q11
Gnaz	GNAZ	22q11.1-q11.2
Col6a1	COL6A1	21q22.3
Col6a2	COL6A2	21q22.3
S100b	S100B	21q22.3
Itgb2	ITGB2	21q22.3
Pfkl	PFKL	21q22.3
Gna15	GNA15	19p13.3
Gna11	GNA11	19p13.3
Tcfe2a	TCF3	19p13.3
Amh	AMH	19p13.3
Pah	PAH	12q22-24.2
Igf1	IGF1	12q22-q23
Tra1	TRA1	12q24.2-qter
Pep2	PEPB	12q21
Mgf	MGF	12q14.3-qter
Myf6	MYF6	12
Myf5	MYF5	12
Lyzs	LYZ	12
Ifg	IFNG	12q24.1
Mdm1	MDM1	12
Gli	GLI	12q13
D10H12S53E	D12S53E	12pter-q21
Erbb3	ERBB3	12q13
	Chromosome 11	
Camk2b	CAMK2B	22q12
Lif	LIF	22q11.1-q13.1
Tcn2	TCN2	22q
Nfh	NEFH	22q12.1-q13.1
Gk	GCK	7p
Ikaros	IKAROS	7p11.2-p13
Erbb	EGFR	7p12
Spnb2	SPTBN1	2p21
Rel	REL	2p13-p12
Hba	HBA1	16p13.3
Adra1	ADRA1A	5q32-q34
Gabra1	GABRA1	5q34-q35
Gabrg2	GABRG2	5q31.1-q33.1
Il4	IL4	5q23-q31
Il5	IL5	5q23-q31
Il3	IL3	5q23-q31
Csfgm	CSF2	5q23-q31
Il13	IL13	5q31
Mgat1	GLCT1	5q31.2-q31.3
Irf1	IRF1	5q23-q31
Camb	ANX6	5q32-q34
Tcf7	TCF7	5q31
Sparc	SPARC	5q31-q33
Glr1	GRM1	5q33
Pmp22	PMP22	17p12-p11.2
Ahd4	ALDH3	17
Myhs	MYH1	17pter-p11
Shbg	SHBG	17pter-p12
Rcvrn	RCV1	17
Myhn2	MYH10	17p13
Zfp3	ZFP3	17pter-p12
Rpo2-1	POLR2	17p13.1
Asgr1	ASGR1	17p13-p11
Asgr2	ASGR2	17p
Acrb	CHRNB	17p12-p11
Trp53	TP53	17p13.1
Atp1b2	ATP1B2	17
Glut4	GLUT4	17p13
D11Bay2	D17S28	17p13.3
Nf1	NF1	17q11.2
Cryba1	CRYBA1	17q11.2-q12
Edp1	EDP	17q22-q23
Tcf2	TCF2	17q11.2-q12
Tca3	SCYA1	17
Sigje	SCYA2	17q11.2-q12
Mip1a	SCYA3	17q11-q21
Mip1b	SCYA4	17q11-q21
Mpo	MPO	17q21.3-q23
Hlf	HLF	17q22
Cola1	COL1A1	17q21.3-q22
Ngfr	NGFR	17q21-q22
Hoxb	HOXB	17q21-q22
Itga3	ITGA3	17
Rara	RARA	17q12
Erbb2	ERBB2	17q11.2-q12
Erba	THRA1	17q11.2-q12
Csfg	CSF3	17q11.2-q12
Top2a	TOP2A	17q21-q22
Krt1	KRT15	17q21-q23
Cnp1	CNP	17q21
Gfap	GFAP	17q21
Itgb3	ITGB3	17q21.32
Wnt3	WNT3	17q21-q22
Mtapt	MAPT	17q21
Myla	MYL4	17q21-qter
Ace	ACE	17q23
Apoh	APOH	17q23-qter
Itga2b	ITGA2B	17q21.32
Empb3	EPB3	17q21-q21
Scn4a	SCN4A	17q23.1-q25.3
Gh	GH1	17q22-q24
Pkca	PRKCA	17q22-q24
Timp2	TIMP2	17q25
Gaa	GAA	17q23
Itgb4	ITGB4	17q11-qter
Glk	GALK1	17q23-q25
Tk1	TK1	17q23.2-q25.3
Thbp	P4HB	17q25
	Chromosome 12	
Pomc1	POMC	2p23
Odc	ODC1	2p25
Apob	APOB	2p24-p23
Synd	SDC	2p
Nmyc1	MYCN	2p24.1
Rrm2	RRM2	2p25-p24
Tpo	TPO	2p25-p24
Ahr	AHHR	2pter-q31
Lamb1-1	LAMB1	7q22-q31
Hspa2	HSPA2	14q22-q24
Pygl	PYGL	14q11.2-q24.3
Max	MAX	14q23
Spnb1	SPTB	14q24.1-q24.2
Fos	FOS	14q24.3
Tshr	TSHR	14q31
Tgfb3	TGFB3	14q24
Galc	GALC	14
Chga	CHGA	14q32
Aat	PI	14q32.1
Pre2	AACT	14q32.1
Cbg	CBG	14-q32.1
D12H14S17	D14S17	14q32.33
Ckb	CKB	14q32.3
IghC	IGH	14q32.33
Akt	AKT1	14q32.33
	Chromosome 13	
Nid	NID	1q43
Rasl1	RALA	7p
Inhba	INHBA	7p15-p13
Tcrg	TCRG	7p15-p14
Gli3	GLI3	7p13
Hist1	H1	6p22.2-p21.1
Pl1	CSH1	17q22-q24
Pl2	CSH2	17q22-q24
Pri	PRL	6p22.2-p21.3
Fim1	FIM1	6p23-p22.3
Bmp6	BMP6	6
D13H6S231E	D6S231E	6p23
Drdl	DRD1	5q34-q35
Il9	IL9	5q22-q32
Srd5a1	SRD5A1	5p15
Nec1	NEC1	5q15-q21
Rasa	RASA	5q13
As1	ARSB	5p11-q13
Crhbp	CRHBP	5q
Dhfr	DHFR	5q11.2-q13.2
Hexb	HEXB	5q13
Mtap5	MAP1B	5q13
Htr1a	HTR1A	5cen-q11
Ctla3	CTLA3	5
Itga1	ITGA1	5
Itga2	ITGA2	5q22-q31
Hmgcr	HMGCR	5q13.3-q14
	Chromosome 14	
Rarb	RARB	3p24
Vcl	VCL	10q22-q23
Plau	PLAU	10q24-qter
Cchl1a2	CACNL1A2	3p14.3
Rbp3	RBP3	10q11.2
Glud	GLUD1	10q21.1-q24.3
Sftp1	SFTP1	10q21-q24
Bmp4	BMP4	14
Apex	APEX	14q11.2-p12
Tcra	TCRA	14q11.2
Tcrd	TCRD	14q11.2
Np1	NP	14q11.2
Ctla1	CTLA1	14q11.2
Ctsg	CTSG	14q11.2
Myhca	MYH6	14q11.2-q13
Myhcb	MYH7	14q112.-q13
Ang	ANG	14q11.1-q11.2
Gjb2	GJB2	13
Gja3	GJA3	13
Nfl	NEFL	8p21
Clu	CLU	8p21
Bmp1	BMP1	8
Sftp2	SFTP2	8p
Gnrh	LHRH	8p21-p11.2
Es10	ESD	13q14.1-q14.2
Htr2	HTR2	13q14-q21
Rb1	RB1	13q14.2
D14H13S26	D13S26	13q21
Rap2a	RAP2A	13q34
Pcca	PCCA	13q32
	Chromosome 15	
Ghr	GHR	5p14-p12
Mlvi2	MLVI2	5p14-p13
Il7r	IL7R	5p13
Prlr	PRLR	5p14-p13
Lifr	LIFR	5p13-p12
C6	C6	5p14-p12
C7	C7	5p14-p12
Hspg	HSPG1	8q22-q23
Myc	MYC	8q24.12-q24.13
Mlvi4	MLVI4	8q24
Pvt1	PVT1	8q24
Tgn	TG	8q24
Gpt1	GPT	8q24.2-qter
Cyp11b	CYP11B	8q21-q22
Il2rb	IL2RB	22q13
Lgals1	LGALS1	22q12-q13.1
Pdgfb	PDGFB	22q12.3-q13.1
Myhn1	MYH9	22q12.3-q13.1
Pva	PVALB	22q12-q13.1
Bzrp	BZRP	22q13.31-qter
Dia1	DIA1	22q13.31-qter
Cyp2d	CYP2D	22q11.2-qter
Acr	ACR	22q13-qter
Pdgfec	ECGF1	22q13
Col2a1	COL2A1	12q12-q13.1
Gdc1	GPD1	12
Wnt1	WNT1	12q13
Ela1	ELA1	12
Cp2	CP2	12
Rarg	RARG	12q13
Itga5	ITGA5	12q11-q13
Hoxc	HOXC	12q12-q13
Itgb7	ITGB7	12q13.1
Krt2	KRT5	12
Spl1	SP1	12q
	Chromosome 16	
Prm1	PRM1	16p13.13
Prm2	PRM2	16p13.13
Igll	IGLL1	12q11.2-q12.3
Igl	IGL	22q11.1-q11.2
Comt	COMT	22q11.1-q11.2
Smst	SST	3q28
Apod	APOD	3q26.2-qter
Stf1	STF1	3q21
Drd3	DRD3	3q13.3
Gap43	GAP43	3q21-qter
Pit1	PIT1	3q
D16H21S16	D21S16	21q11
D16H21S52	D21S52	21q11
App	APP	21q21.2
Glur5	GLUR5	21q21.1-q22.1
Sod1	SOD1	21q22.1
D16H21S58	D21S58	21q22.1-q22.2
Gart	GART	21q22.1
Ifrc	IFNAR	21q22.1
Son	SON	21q22.1
Cbr	CBR	21
Pcp4	PCP4	21
Erg	ERG	21q22.3
Ets2	ETS2	21q22.3
Mx1	MX1	21q22.3
Mx2	MX2	21q22.3
Hmg14	HMG14	21q22.3
	Chromosome 17	
Mas1	MAS	6q24-q27
Igf2r	IGF2R	6q25-q27
Tcp10a	TCP10A	6q27
Plg	PLG	6q26-q27
Tcp1	TCP1	6q25-q27
Sod2	SOD2	6q25
Tcp10b	TCP10B	6q27
Tcp10c	TCP10A	6q27
Thbs2	THBS2	6q27
Tcte3	TCTE3	6q27
D17Lon1	N.A.	16p13.3
D17Lon2	N.A.	16p13.3
Cbs	CBS	21q22.3
Crya1	CRYAA	21q22.3
D17H21S56	D21S56	21q22.3
Pim1	PIM1	6p21
Glo1	GLO1	6p21.3-p21.1
H2	HLA	6p21.3
Tnfa	TNFA	6p21.3
Rps18	RPS18	6p21.3
Col11a2	COL11A2	6p21.3
Cyp21a1	CYP21	6p21.3
C4	C4	6p21.3
Cyp21a2ps	CYP21P	6p21.3
Rd	RD	6p21.3
Bf	BF	6p21.3
Bat1	BAT1	6p21.3
C2	C2	6p21.3
Neu1	NEU	6
Hsp70	HSPA1	6p21.3
Tnfb	TNFB	6p21.3
Rxrb	RXRB	6pter-q13
Pgk2	PGKB	6p21.1-p12
Mut	MUT	6p2
Tpx1	TPX1	6p21-qter
Tcte1	TCTE1	6p21
Nfya	NFYA	6p21.1
Rd2	RDS	6p21.2-cen
Upg1	PGC	6pter-p21.1
C3	C3	19p13.3-p13.2
Vav	VAV	19p13.2
Fert	FER	5q21
Lama	LAMA	18p11.32-p11.2
Tik	TIK	2p22-p21
Lhcgr	LHCGR	2p21
	Chromosome 18	
Nil2	NIL2	10p11.2
Tpl2	TPL2	10p11
Ncad	NCAD	18q12.1
Ttr	TTR	18q12.1
spm	NPC	18p
Apc	APC	5q21-q22
Egr1	EGR1	5q23-q31
Camk4	CAMK4	5q21-q23
Fgf1	FGF1	5q31.3-q33.2
Grl1	GRL	5q31-q32
Mcc	MCC	5q21-q22
Lox	LOX	5q23.3-q31.2
Ii	CD74	5q31-q33
Pdgfrb	PDGFRB	5q33-q35
Csfmr	CSF1R	5q33-q35
Rps14	RPS14	5q31-q33
Adrb2	ADRB2	5q31-q32
Pdea	PDEA	5q31.2-q34
Fech	FECH	18q21.2-q21.3
Grp	GRP	18q21.1-q21.32
Dcc	DCC	18q21.1
Mbp	MBP	18q23
	Chromosome 19	
Adrbk1	ADRBK1	11q13
Pcx	PCX	11q
Gst3	GSTP1	11q13
Seao	SEA	11q13

Mouse Symbol	Human Symbol	Human Location
Mdu1	MDU1	11q12-q13
Pygm	PYGM	11q12-q13.2
Fth	FTH1	11q13
Cd5	CD5	11q13
Cntf	CNTF	11
Cd20	CD20	11q12-q13.1
Osbp	OSBP	11q11-qter
Ahd2	ALDH1	9q21
Lpc1	ANX1	9q12-q21.2
Rln	RLN1	9pter-q12
Fas	APT1	10q23-q24.1
Ide	IDE	10q23-q25
Got1	GOT1	10q24.1-q25.1
Cyp2c	CYP2C	10q24.1-q24.3
Rbp4	RBP4	10q23-q24
Tdt	DNTT	10q23-q24
Notch1	HOX11	10q24
Bpag2	BPAG2	10q24.
Adra2a	ADRA2A	10q24-q26
Adrb1	ADRB1	10q24-q26
Cyp17	CYP17	10q24.3
Csfgmra	CSF2RA	Xp22.32; Yp11.3
	Chromosome X	
Gata1	GATA1	Xp11.23
Cybb	CYBB	Xp21.1
Otc	OTC	Xp21.1
Td	IP1	Xp11.21-cen
DXHXS32	DXS32	Xp22-p11
DXHXS676	DXS676	Xp21.1-p11.3
Ubelx	UBE1	Xp11.23
Maoa	MAOA	Xp11.4-p11.3
Maob	MAOB	Xp11.4-p11.3
Timp	TIMP1	Xp11.3-p11.23
Syn1	SYN1	Xp11.23
Pfc	PFC	Xp11.3-p11.23
Araf	ARAF1	Xp11.3-p11.23
Lamp2	LAMP2	Xq24
Hprt	HPRT	Xq26.1
Cd40l	CD40L	Xq26
Cf9	F9	Xq26.3-27.1
Mcf2	MCF2	Xq26.3-27.1
Cdr	CDR1	Xq27.1-q27.2
Fmr1	FMR1	Xq27.3
DXHXS296	DXS296	Xq27.3-q28
Ids	IDS	Xq27.3-q28
Gabra3	GABRA3	Xq28
DXHXS1104	DXS1104	Xq28
Bpa	CDPX2	X
Str	IP2	Xq27-q28
DXPas8	DXS52	Xq28
Bgn	BGN	Xq28
L1cam	L1CAM	Xq28
Avpr2	AVPR2	Xq28
DXHXS254E	DXS254E	Xq28
DXHXS253E	DXS253E	Xq28
G6pd	G6PD	Xq28
Psvp	RCP	Xq28
Cf8	F8C	Xq28
Dmd	DMD	Xp21.3-p21.2
Pola	POLA	Xp21.1-p21.3
Zfx	ZFX	Xp22.1
Ar	AR	Xq11.2-q12
Ta	EDA	Xq12-q13.1
Gjb1	GJB1	Xq13.1
Ccg1	CCG1	Xq13.1
Rps4x	RPS4X	Xq13.1
Phka1	PHKA1	Xq13.1
DXHXS393	DXS393	Xq13-q24
Xist	XIST	Xq13.2
Pgk1	PGK1	Xq13.3
Btk	BTK	Xq21.33-q22
Ags	GLA	Xq21.33-q22
Plp	PLP	Xq21.33-q22
DXHXS101	DXS101	Xq22
DXHXS178	DXS178	Xq21.33-q22
Prps1	PRPS1	Xq21-q27
Col4a5	COL4A5	Xq22
Alas2	ALAS2	Xp11.21
DXHXS674	DXS674	Xp11.22-p11.21
DXHXS679	DXS679	Xp11.22-p11.21
Pdha1	PDHA1	Xp22.1
Glra2	GLRA2	Xp22.1-p21.3
PrpS2	PRPS2	Xp22.3-p22.2
Grpr	GRPR	Xp11.22-cen
Amel	AMELX	Xp22.31-p22.1
Sts	STS	Xp22.32

*Human chromosomal locations for most loci were obtained from GDB, a computerized database of human linkage information maintained by the William H. Welch Medical Library (The Johns Hopkins University, Baltimore, MD). The human mapping results for a few of the loci have yet to be published, and we thank the many laboratories who have given us permission to cite their unpublished mapping data. N.A., not assigned.

ping can be found in the evolution of the homeobox genes (*25*).

Mapping can also provide unexpected insights into chromosome evolution. For example, although the X chromosome tends to show extreme conservation of genes across mammalian species, Disteche *et al.* (*26*) recently showed that the mouse granulocyte-macrophage colony-stimulating factor receptor α subunit gene (*Csfgmra*), which is located in the pseudoautosomal region of the X and Y chromosomes in humans, maps to the very distal region of mouse chromosome 19. This was the first demonstration of a gene that is pseudoautosomal in humans but not in mice. This finding may not be surprising, however, because it is known that genes in the pseudoautosomal region have homologs on both the X and Y chromosomes and are likely to escape X inactivation (*26*); the process of X inactivation is thought to be responsible for the conservation of genes on the mammalian X chromosome.

Cloning classical mouse mutations. Over the past century, hundreds of mutations that cause deviant phenotypes have been identified and characterized in the mouse. These mutations represent spontaneous mutations, as well as mutations induced by chemicals, radiation, transgene insertion, viral integration, and more recently, homologous recombination in embryonic stem (ES) cells. Although it is obvious that many of these mutations define a set of developmentally important genes, few of the mutant genes have been cloned, with the exception of those mutations induced by homologous recombination in ES cells.

Mouse linkage maps are already having a great impact on the rate at which these mutations are cloned. In Table 2, we have compiled a list (albeit probably incomplete) of mouse mutations that have been successfully cloned. Most of these mutations (31 of 42) were cloned by the candidate gene approach, which works as follows: As each new gene is placed on the mouse map, phenotypic deviants mapping in the vicinity can be reviewed to determine if any has a phenotype consistent with what one might expect to result from a defect in the mapped gene. If a plausible connection is found, the gene in question can be molecularly characterized in both wild-type and deviant mice for the identification of mutations. Given the rapid expansion of the gene-based map, it is likely that many more mutations will be cloned in the future by means of the candidate gene approach.

Several mouse mutations (5 of 42) were cloned after one or more alleles were found that are molecularly tagged with a transgene insertion, viral sequence, or genome rearrangement (Table 2). Again, one of the first steps in this cloning approach is to map sequences from the tagged allele in order to determine if any mutations exist that map in the same vicinity and that have a phenotype similar to that of the molecularly tagged allele. Complementation tests for recessive and semidominant deviants can then be performed to determine if the molecularly tagged allele is allelic with any preexisting mutations. The molecular tag can then be used as an entry point for cloning the mutated gene.

Several other mutations have been cloned by positional cloning (4 of 42)—that is, chromosomal walking from nearby genetic markers (Table 2) (*27*). Until very recently, this approach was largely impractical because of the paucity of molecular markers on the mouse genetic map and the absence of efficient walking methods and large insert libraries. However, given the great increase in marker density on current mouse genetic maps, particularly with respect to SSLP markers, and given the availability of large-insert yeast artificial chromosome (YAC) libraries of the mouse genome (*28*), it is now possible to positionally clone virtually any mouse mutation. The rate-limiting steps in positional cloning have now become the generation of large numbers of backcrossed animals needed to define recombination events in close proximity to the mutation of interest and the identification and evaluation of candidate genes in the nonrecombinant interval, rather than the identification of closely linked markers. As physical maps of the mouse genome become available and techniques for identifying genes in large blocks of genomic DNA improve, the ability to clone mutations on the basis of their position will be enhanced.

Two classical spontaneous mutations were cloned serendipitously as an indirect result of attempts to generate germ-line knock-out mutations in the transforming growth factor α (*Tgfa*) and wingless-related mouse mammary tumor virus (MMTV) integration site–1 (*Wnt-1*) genes. Knock-out mutations in these two genes produced phenotypes very similar to those of the spontaneous mutations waved-1 (*wa-1*) and swaying (*sw*), respectively. Complementation tests showed that the classical mutations were allelic to the knock-out mutations, and molecular studies confirmed that the spontaneous mutations resulted from defects in these genes. Given the rapid rate at which new genes are being knocked-out by homologous recombination, it is likely that other classical mutations will be cloned by this approach as well. Again, maps and phenotypic comparisons will continue to provide the crucial clues.

Mouse models of human genetic diseases. The mouse has provided many important models of human genetic diseases. In the chart, we have provided a partial list of known single-gene models of human genetic diseases as well as polygenic disorders that may also be models for certain human conditions. Even with such a partial list, it is obvious that the number of known or

potential mouse models of human diseases is large and includes some of the most important diseases affecting humans. Not included in this list are many uncloned mouse mutations that are also thought to represent models for human diseases (29). As discussed earlier, the development of a high-density linkage map of the mouse genome will greatly increase the speed at which these mutations are cloned and hence facilitate the development of additional models of human diseases. Once human disease genes are cloned and mutations characterized, further research on gene function and disease will rely in part on mouse models.

Mapping genes in the mouse can also facilitate the cloning of human genetic disease loci, even in cases where no appropriate mouse model exists. For example, given the speed at which new genes can be mapped in the mouse, the high density of the mouse linkage map, and the considerable amount of information already gained regarding human-mouse comparative mapping, it is often easier to map a new gene in the mouse and predict its location in humans than to map the gene directly in humans. In some cases, the predicted location may lie near an already mapped human disease locus and subsequent studies may show that defects in that gene are in fact responsible for the disease (30).

Prospects for the Future

The advent of dense genetic linkage maps and other technological advances not only simplifies traditional mouse genetic studies, but also opens up completely new paradigms and approaches. Although it is hard to predict the full range of future directions, some areas seem poised for rapid expansion in the coming years.

Genetic dissection of polygenic traits. With the genetic analysis of single-gene traits becoming increasingly straightforward, the challenging frontier will begin to shift to the study of polygenic traits that provide models of common human diseases. Mouse strains show striking variation in their susceptibility to diabetes, epilepsy, cancer, bacterial and viral infections, and obesity (31). There is also substantial inherited variation in such physiological parameters as skeletal morphology, blood pH, response to drugs and hormone treatments, immunological responses, life-span, and behavior (31). In most cases, these differences are the result of the combined effects of multiple, interacting genes. Genetic dissection of such polygenic traits requires simultaneously following the inheritance of markers spanning the entire genome to identify the regions that together account for the phenotype (32). This has only just become practical with the advent of dense genetic maps, particularly that of the easily typed and highly polymorphic SSLPs. Some early studies have confirmed the promise of this approach. Some (33) have undertaken a comprehensive genetic dissection of the factors causing type 1 diabetes in the nonobese diabetic (NOD) mouse. Frankel and co-workers (34) have dissected genetic factors underlying epilepsy in a seizure-prone strain. Dietrich and colleagues (35) have analyzed the severity of colon cancer in mice that carry a mutation in the *Apc* gene (the homolog of the human gene underlying familial colon cancer) and mapped a major quantitative modifier locus that dramatically alters the phenotype. Similarly, others (36) have shown the power of using recombinant congenic strains to analyze polygenic variation in cancer susceptibility. Quantitative variation may prove especially valuable for the study of mammalian physiology, not least because it is easier to find such variation than to identify single-gene

Table 2. Representative mouse phenotypic deviants for which the altered genes have been identified.

Cloning Mechanism	Mutation	Chromosomal Location	Gene	Reference
Candidate Gene	Adipose storage deficiency (*ads*) [mucopolysaccharidosis typeVII (*gus* ^{mps})]	5	Beta-glucuronidase	40
	Albino (*c*)	7	Tyrosinase	41
	Arrested development of righting response (*adr*)	6	Skeletal muscle chloride channel	42
	Brown (*b*)	4	Tyrosinase related protein	43
	Dominant spotting (*W*)	5	Kit protooncogene	44
	Dwarf (*dw*)	16	Pituitary transcription factor-1	45
	Extension locus (*E*)	8	Melanocyte stimulating hormone receptor	46
	Extra toes (*Xt*)	13	Gli-Kruppel family member 3	47
	Jimpy (*jp*)	X	Myelin proteolipid protein	48
	Little (*lit*)	6	Growth hormone releasing factor receptor	49
	Lymphoproliferation (*lpr*)	19	Fas antigen	50
	Motheaten (*me*)	6	Hematopoietic cell phosphatase	51
	Multiple intestinal neoplasia (*Min*)	18	Adenomatous polyposis coli	52
	Muscular dysgenesis (*mdg*)	1	Alpha 1 dihydropyridine sensitive calcium channel receptor	53
	Muscular dystrophy, X-linked (*mdx*)	X	Dystrophin	54
	Myxovirus sensitivity (*Mx*)	16	Mx protein	55
	Osteopetrosis (*op*)	3	Colony stimulating factor, macrophage	56
	Pallid (*pa*)	2	Pallidin (Epb 4.2)	57
	Retinal degeneration (*rd*)	5	cGMP-phosphodiesterase, beta subunit	58
	Retinal degeneration slow (*Rd2*)	17	Photoreceptor peripherin	59
	Shiverer (*shi*)	18	Myelin basic protein	60
	Slaty (*slt*)	14	Tyrosinase related protein 2	61
	Small eye (*Sey*)	2	Paired box gene 6	62
	Sparse fur (*spf*)	X	Ornithine transcarbamylase	63
	Splotch (*Sp*)	1	Paired box gene 3	64
	Steel (*Sl*)	10	Mast cell growth factor	65
	Testicular feminization (*Tfm*)	X	Androgen receptor	66
	Testis determining Y (*Tdy*)	Y	*Sry* transcription factor	67
	Trembler (*Tr*)	11	Peripheral myelin protein, 22kD	68
	Undulated (*un*)	2	Paired box homeotic gene-1	69
	X-linked immune deficiency (*xid*)	X	Burton's tyrosine kinase	70
Insertion Tags	Dilute (*d*)	9	Novel myosin heavy chain	71
	Limb deformity (*ld*)	2	Formin	72
	Pink-eyed dilution (*p*)	7	P polypeptide	73
	Microphthalmia (*mi*)	6	Mi bHLHZip protein	74
	Moloney leukemia virus 13 (*Mov13*) integration site	11	Procollagen type I alpha 1	75
Positional Cloning	Agouti (*a*)	2	Agouti signal protein	76
	Brachyury (*T*)	17	T product	77
	Mycobacterium bovis resistance (*Bcg*)	1	Nramp transporter	78
	Short-ear (*se*)	9	Bone morphogenetic protein 5	79
ES cell-induced mutation	Swaying (*sw*)	15	Wingless related MMTV integration site 1	80
	Waved-1 (*wa1*)	6	Transforming growth factor, alpha	81

mutants with dramatic phenotypes (presumably because missense variants may be tolerated, whereas null alleles in key physiological processes may be lethal). Moving from initial linkage to cloned loci for such polygenic traits remains a challenge for the future, but strategies have been outlined and several projects are under way.

Deletion analysis of tumors. A powerful approach in cancer research has been the identification of chromosomal regions that undergo genetic changes, such as deletions, mitotic recombination, or chromosomal loss and reduplication, during tumor initiation and progression. Such regions can be recognized because genetic markers that are heterozygous in normal tissue are reduced to homozygosity by these structural alterations. Genome-wide loss-of-heterozygosity (LOH) studies have been carried out for a number of tumor types in humans, but they have not yet become common in the mouse. With the availability of dense genetic maps, this situation is likely to change.

Mice offer great advantages for LOH mapping compared to humans. F_1 hybrid mice between two strains can provide an unlimited number of tumors from a genetically defined background that can all be typed with a single set of fully informative markers. The use of F_1 hybrids eliminates the effect of genetic background; this is unlike the situation in human studies, where one cannot typically tell whether variation in LOH among patients is due to chance or inherited differences affecting the process of tumorigenesis. In mice, one can also study whether one allele is preferentially lost in the F_1 hybrids, which suggests that the opposite chromosome carries a linked locus predisposing to cancer; such assessments are impossible in outbred populations such as that of humans. Moreover, in mice tumor progression can be analyzed by examining tumors at various histological stages. Finally, fine-structure deletion mapping and positional cloning of tumor suppressor genes in mice should be feasible, given the ability to collect hundreds of tumors. With a wide range of naturally occurring, chemically induced, and transgene-induced tumors available, the mouse is ideal for genetic studies of tumorigenesis in vivo.

Physical maps, gene catalogs, and genomic sequences. Over the next decade, mouse genome mapping will continue at a rapid pace. One early target will surely be construction of a complete physical map of the mouse genome. Although the mouse genome is the same size as the human genome, the task of physical mapping is simplified by the ease of ordering anchor points by genetic mapping. Indeed, a physical map should virtually fall out as the density of markers in the genetic map increases. The current genetic map with 1500 SSLPs has an average spacing between markers of about 2 Mb, which corresponds to about three, large-insert (~700 kb) YACs from available libraries (*28*). With projects under way to create a map of 6000 SSLPs, the average spacing should fall to about 500 kb, with the result that most of the physical map may be constructed simply by identifying the YACs corresponding to each consecutive marker along a chromosome (*37*).

A subsequent milestone will be the identification of all mouse genes and their localization on the genetic and physical maps. With improved methods for generating "normalized" complementary DNA (cDNA) libraries, it may become practical to catalog genes from all developmental stages and most adult organs by complete cDNA sequencing and PCR-based mapping of the cDNAs to YACs. A natural extension of today's gene-based map, such a catalog should prove invaluable for studies involving positional cloning, human-mouse comparison, and genome organization.

Finally, the recently revised goals of the Human Genome Project include obtaining the complete nucleotide sequences of both the human and mouse genomes. By comparing two mammalian genomes, important regions should become obvious by virtue of their sequence conservation over 140 million years of evolution. Already, comparative sequencing of the T cell receptor regions in humans and mice has revealed many novel regulatory signals (*38*). Although the notion of sequencing two mammalian genomes might seem prohibitively costly, it seems likely that DNA sequencing technology either will advance to the point that both genomes can be easily sequenced or will fall short of accommodating even a single genome; it is implausible that it will be feasible to sequence one but not both.

Conclusion

Mouse genetics began several hundred years ago, with the cultivation of coat color and neurological mutants whose odd colors and behaviors entertained the imperial courts of Japan (*39*). Over the past half century, the mouse has become a mainstay of biomedical research in areas ranging from embryology to immunology. As mouse genetics enters the next millenium, it is clear that the field will continue to provide an ever deeper window into ourselves through the many similarities in our physiology, our heritable diseases, and, ultimately, our genomes.

REFERENCES AND NOTES

1. J. B. S. Haldane, A. D. Sprunt, N. M. Haldane, *J. Genet.* **5**, 133 (1915).
2. E. M. Eicher, in *Mammalian Genetics and Cancer: The Jackson Laboratory Fiftieth Anniversary Symposium*, E. S. Russell, Ed. (Liss, New York, 1981), pp. 7–49.
3. D. Botstein, *Am. J. Hum. Genet.* **32**, 314 (1980).
4. B. A. Taylor, in *Genetic Variants and Strains of the Laboratory Mouse*, M. F. Lyon and A. G. Searle, Eds. (Oxford Univ. Press, Oxford, 1989), pp. 773–796.
5. F. Bonhomme, F. Benmehdi, J. Britton-Davidian, S. Martin, *C. R. Acad. Sci. Paris* **289**, 545 (1979).
6. P. Avner, L. Amar, L. Dandolo, J. L. Guénet, *Trends Genet.* **4**, 18 (1988).
7. *Mammalian Genome 4 (Suppl.)*, L. M. Silver, J. H. Nadeau, P. Goodfellow, Eds. (Springer-Verlag, New York, in press); *Mouse Genome*, J. Peters, Ed. **91**, 19 (1993); GBASE, a computerized database of mouse linkage information maintained by The Jackson Laboratory, Bar Harbor, ME.
8. N. G. Copeland and N. A. Jenkins, *Trends Genet.* **7**, 113 (1991); unpublished results.
9. J. D. Ceci *et al.*, unpublished results.
10. J. L. Weber, *Genomics* **7**, 524 (1990); _____ and P. E. May, *Am. J. Hum. Genet.* **44**, 388 (1989).
11. C. M. Hearn *et al.*, *Mamm. Genome* **1**, 273 (1991); J. M. Love, A. M. Knight, M. A. McAleer, J. A. Todd, *Nucleic Acids Res.* **18**, 4123 (1990); R. J. Cornall, T. J. Aitman, C. M. Hearn, J. A. Todd, *Genomics* **10**, 874 (1991).
12. W. Dietrich *et al.*, *Genetics* **131**, 423 (1992); W. Dietrich *et al.*, in *Genetic Maps*, S. J. O'Brien, Ed. (Cold Spring Harbor Laboratory Press, Cold Spring Harbor, NY, ed. 6, 1993), pp. 4.110–4.142.
13. E. S. Lander *et al.*, *Genomics* **1**, 174 (1987).
14. S. E. Lincoln and E. S. Lander, *ibid.* **14**, 604 (1992).
15. E. J. Zimmer, E. Ogin, D. C. Shreffler, H. C. Passmore, *Immunogenetics* **25**, 274 (1987); Y. Uematsu, H. Kiefer, R. Schulze, K. Fischer-Lindahl, M. Steinmetz, *EMBO J.* **5**, 2121 (1986); T. Shiroishi *et al.*, *Immunogenetics* **31**, 79 (1990); J. A. Kobori, E. Strauss, K. Minard, L. Hood, *Science* **234**, 173 (1986); R. H. Reeves, M. R. Crowley, B. F. O'Hara, J. D. Gehart, *Genomics* **8**, 141 (1990); R. H. Reeves, M. R. Crawley, W. S. Moseley, M. F. Seldin, *Mamm. Genome* **1**, 158 (1991).
M. T. Davisson, T. H. Roderick, D. P. Doolittle, in *Genetic Variants and Strains of the Laboratory Mouse*, M. F. Lyon and A. G. Searle, Eds. (Oxford Univ. Press, Oxford, 1989), pp. 432–505.
17. M. F. Hammer, J. Schimenti, L. M. Silver, *Proc. Natl. Acad. Sci. U.S.A.* **86**, 3261 (1989).
18. F. G. Biddle, *Genome* **29**, 389 (1987).
19. J. D. Ceci, L. D. Siracusa, N. A. Jenkins, N. G. Copeland, *Genomics* **5**, 699 (1989); M. J. Justice *et al.*, *Genetics* **125**, 855 (1990); L. D. Siracusa, A. M. Buchberg, N. G. Copeland, N. A. Jenkins, *ibid.* **122**, 669 (1989).
20. J. H. Nadeau and B. A. Taylor, *Proc. Natl. Acad. Sci. U.S.A.* **81**, 814 (1984).
21. O. Hino *et al.*, *ibid.* **90**, 730 (1993).
22. S. J. O'Brien *et al.*, *Nature Genet.* **3**, 103 (1993).
23. J. H. Nadeau, in *Advanced Techniques in Chromosome Research*, K. W. Adolph, Ed. (Marcell Dekker, New York, 1991), pp. 269–296; K. Schughart, C. Kappen, F. H. Ruddle, *Proc. Natl. Acad. Sci. U.S.A.* **86**, 7067 (1989); L. G. Lundin, *Genomics* **16**, 1 (1993).
24. T. M. Wilkie *et al.*, *Nature Genet.* **1**, 85 (1992).
25. R. Krumlauf, *BioEssays* **14**, 245 (1992); P. Hunt and R. Krumlauf, *Annu. Rev. Cell Biol.* **8**, 227 (1992); R. Krumlauf, *Trends Genet.* **9**, 106 (1993); J. W. Pendleton, B. K. Nagai, M. T. Martha, F. H. Ruddle, *Proc. Natl. Acad. Sci. U.S.A.* **90**, 6300 (1993); J. H. Nadeau, J. G. Compton, V. Giguère, J. Rossant, S. Varmuza, *Mamm. Genome* **3**, 202 (1992).
26. C. M. Disteche *et al.*, *Nature Genet.* **1**, 333 (1992).
27. F. S. Collins, *ibid.*, p. 3.
28. Z. Larin, A. P. Monaco, H. Lehrach, *Proc. Natl. Acad. Sci. U.S.A.* **88**, 4123 (1991); K. Kusumi *et al.*, *Mamm. Genome* **4**, 391 (1993); F. L. Chartier, *Nature Genet.* **1**, 132 (1992).
29. J. R. Buchhalter, *Epilepsia* **34**, S31 (1993); J. E. Dick, *Mol. Genet. Med.* **1**, 77 (1991); S. M. Darling and C. M. Abbott, *BioEssays* **14**, 359 (1992); M. C. Johnston and P. T. Bronsky, *J. Craniofacial Genet. Dev. Biol.* **11**, 277 (1991); J. E. Dick, F. Pflumio, T.

Lapidot, *Semin. Immunol.* **3**, 367 (1991); J. P. Sundberg, W. G. Beamer, L. D. Shultz, R. W. Dunstan, *J. Invest. Dermatol.* **95**, 62S (1990); R. S. Fisher, *Brain Res. Rev.* **14**, 245 (1989); J. Hardy, *Trends Neurosci.* **11**, 89 (1988); J. M. Holland, *Clin. Dermatol.* **6**, 159 (1988); E. H. Leiter *et al.*, *Birth Defects* **23**, 221 (1987).
30. S. E. Leff *et al.*, *Nature Genet.* **2**, 259 (1992); T. Özçelik *et al.*, *ibid.*, p. 265; R. Cutler Allen *et al.*, *Science* **259**, 990 (1993); C. T. Baldwin *et al.*, *Nature* **355**, 637 (1992); M. Tassabehji *et al.*, *ibid.*, p. 635; M. Tassabehji *et al.*, *Nature Genet.* **3**, 26 (1993).
31. M. F. W. Festing, *Inbred Strains in Biomedical Research* (Oxford Univ. Press, New York, 1979).
32. A. H. Paterson *et al.*, *Nature* **335**, 721 (1988); E. S. Lander and D. Botstein, *Genetics* **121**, 185 (1989).
33. J.-B. Prins *et al.*, *Science* **260**, 695 (1993); J. A. Todd *et al.*, *Nature* **351**, 542 (1991); R. J. Cornall *et al.*, *ibid.* **353**, 262 (1991).
34. M. L. Rise, W. N. Frankel, J. M. Coffin, T. N. Seyfried, *Science* **253**, 669 (1991).
35. W. F. Dietrich *et al.*, *Cell*, in press.
36. P. C. Groot *et al.*, *FASEB J.* **6**, 2826 (1992); C. J. Moen *et al.*, *Mamm. Genome* **1**, 217 (1991).
37. R. Arratia, E. S. Lander, S. Tavare, M. Waterman, *Genomics* **11**, 806 (1991).
38. L. Hood, personal communication.
39. M. Tokuda, *J. Hered.* **26**, 481 (1935).
40. E. Birkenmeier *et al.*, *J. Clin. Invest.* **83**, 1258 (1989).
41. B. S. Kwon, A. K. Haq, S. H. Pomerantz, R. Halaban, *Proc. Natl. Acad. Sci. U.S.A.* **84**, 7473 (1987).
42. K. Steinmeyer *et al.*, *Nature* **354**, 304 (1991).
43. I. J. Jackson, *Proc. Natl. Acad. Sci. U.S.A.* **85**, 4392 (1988).
44. B. Chabot, D. A. Stephenson, V. M. Chapman, P. Besmer, A. Bernstein, *Nature* **335**, 88 (1988); E. N. Geissler, M. A. Ryan, D. E. Housman, *Cell* **55**, 185 (1988).
45. S. Li *et al.*, *Nature* **347**, 528 (1990); S. A. Camper, T. L. Saunders, R. W. Katz, R. H. Reeves, *Genomics* **8**, 586 (1990).
46. L. S. Robbins *et al.*, *Cell* **72**, 827 (1993).
47. T. Schimmang, M. Lemaistre, A. Vortkamp, U. Rutter, *Development* **116**, 799 (1992); C.-C. Hui and A. L. Joyner, *Nature Genet.* **3**, 241 (1993).
48. A. Dautigny *et al.*, *Nature* **321**, 867 (1986).
49. P. Godfrey *et al.*, *Nature Genet.* **4**, 227 (1993); S.-C. Lin *et al.*, *Nature* **364**, 208 (1993).
50. R. Watanabe-Fukunaga, C. I. Brannan, N. G. Copeland, N. A. Jenkins, S. Nagata, *Nature* **356**, 314 (1992).
51. H. W. Tsui, K. A. Siminovitch, L. de Souza, F. W. L. Tsui, *Nature Genet.* **4**, 124 (1993); L. D. Shultz *et al.*, *Cell* **73**, 1445 (1993).
52. L.-K. Su *et al.*, *Science* **256**, 668 (1992).
53. T. Tanabe, K. G. Beam, J. A. Powell, S. Numa, *Nature* **336**, 134 (1988).
54. E. P. Hoffman, R. H. Brown, L. M. Kunkel, *Cell* **51**, 919 (1987); P. Sicinski *et al.*, *Science* **244**, 1578 (1989).
55. P. Staeheli, R. Grob, E. Meier, J. G. Sutcliffe, O. Haller, *Mol. Cell. Biol.* **8**, 4518 (1988); H. Arnheiter, S. Skuntz, M. Noteborn, S. Chang, E. Meier, *Cell* **62**, 51 (1990).
56. H. Yoshida *et al.*, *Nature* **345**, 442 (1990).
57. R. A. White *et al.*, *Nature Genet.* **2**, 80 (1992).
58. C. Bowes *et al.*, *Nature* **347**, 677 (1990).
59. G. H. Travis, M. B. Brennan, P. E. Danielson, C. A. Kozak, J. G. Sutcliffe, *Nature* **338**, 70 (1989); G. Connell, *Proc. Natl. Acad. Sci. U.S.A.* **88**, 723 (1991).
60. C. Readhead *et al.*, *Cell* **48**, 703 (1987).
61. I. J. Jackson *et al.*, *EMBO J.* **11**, 527 (1992).
62. R. E. Hill *et al.*, *Nature* **354**, 522 (1991).
63. G. Veres, R. A. Gibbs, S. E. Scherer, C. T. Caskey, *Science* **237**, 415 (1987).
64. D. J. Epstein, M. Vekemans, P. Gros, *Cell* **67**, 767 (1991).
65. N. G. Copeland *et al.*, *ibid.* **63**, 175 (1990); E. Huang *et al.*, *ibid.*, p. 225; K. M. Zsebo *et al.*, *ibid.*, p. 213.
66. M.-L. Gaspar, T. Meo, P. Bourgarel, J.-L. Guenet, M. Tosi, *Proc. Natl. Acad. Sci. U.S.A.* **88**, 8606 (1991); N. J. Charest *et al.*, *Mol. Endocrinol.* **5**, 573 (1991).
67. J. Gubbay *et al.*, *Nature* **346**, 245 (1990).
68. U. Suter *et al.*, *ibid.* **356**, 241 (1992); U. Suter *et al.*, *Proc. Natl. Acad. Sci. U.S.A.* **89**, 4382 (1992).
69. R. Balling, U. Deutsch, P. Gruss, *Cell* **55**, 531 (1988).
70. D. J. Rawlings *et al.*, *Science* **261**, 358 (1993); J. D. Thomas *et al.*, *ibid.*, p. 355.
71. J. A. Mercer, P. K. Seperack, M. C. Strobel, N. G. Copeland, N. A. Jenkins, *Nature* **349**, 709 (1991).
72. R. P. Woychik, T. A. Stewart, L. G. Davis, P. D'Eustachio, P. Leder, *ibid.* **318**, 36 (1985); R. P. Woychik, R. L. Maas, R. Zeller, T. F. Vogt, P. Leder, *ibid.* **346**, 850 (1990).
73. M. H. Brilliant, Y. Gondo, E. M. Eicher, *Science* **252**, 566 (1991); J. M. Gardner *et al.*, *ibid.* **257**, 1121 (1992); E. M. Rinchik *et al.*, *Nature* **361**, 72 (1993).
74. C. A. Hodgkinson *et al.*, *Cell* **74**, 395 (1993).
75. A. Schnieke, K. Harbers, R. Jaenisch, *Nature* **304**, 315 (1983).
76. S. J. Bultman, E. J. Michaud, R. P. Woychik, *Cell* **71**, 1195 (1992); M. W. Miller *et al.*, *Genes Dev.* **7**, 454 (1993).
77. B. G. Herrmann, S. Labeit, A. Poustka, T. R. King, H. Lehrach, *Nature* **343**, 617 (1990).
78. S. M. Vidal, D. Malo, K. Vogan, E. Skamene, P. Gros, *Cell* **73**, 469 (1993).
79. D. M. Kingsley *et al.*, *ibid.* **71**, 399 (1992).
80. K. R. Thomas, T. S. Musci, P. E. Neumann, M. R. Capecchi, *ibid.* **67**, 969 (1991).
81. N. C. Luetteke *et al.*, *ibid.* **73**, 263 (1993); G. B. Mann *et al.*, *ibid.*, p. 249.
82. We thank all of the mouse chromosome committee chairpersons who reviewed the gene maps. We also thank investigators who supplied probes and reagents as well as those who allowed us to cite unpublished results. Finally, we thank past and present students, postdoctoral fellows, and technicians who have aided in the development of these maps. This work was supported in part by the National Cancer Institute under contract NO1-CO-74101 with ABL (N.G.C., D.J.G., and N.A.J.) and by the National Center for Human Genome Research, grant HG00198 (E.S.L.).